# Metabolism of halauxifen acid is regulated by genes located on wheat chromosome 5A

Olivia A. Landau[1] , Jeanaflor Crystal T. Concepcion[2] and Dean E. Riechers[3]

[1]Graduate Research Assistant, Department of Crop Sciences, University of Illinois, Urbana, IL, USA; [2]Postdoctoral Research Associate, Department of Crop Sciences, University of Illinois, Urbana, IL, USA and [3]Professor, Department of Crop Sciences, University of Illinois, Urbana, IL, USA

## Abstract

Allohexaploid wheat (*Triticum aestivum* L.) is tolerant to halauxifen-methyl (HM) via rapid detoxification of the phytotoxic form of HM, halauxifen acid (HA), to non-phytotoxic metabolites. Previous research utilizing 'Chinese Spring' (CS) wheat, alien substitution (i.e., endogenous chromosome pair substituted with a homoeologous pair from diploid Sears' goatgrass (*Aegilops searsii* M. Feldman & M. Kislev) (AS), or nullisomic-tetrasomic (NT) lines indicated plants lacking chromosome 5A are more sensitive than CS to HM. We hypothesized the increased HM sensitivity of these plants results from losing gene(s) on chromosome 5A associated with HA metabolism, which leads to a reduced HA detoxification rate relative to CS. To compare HA abundance among AS, CS, alien substitution, and NT lines during a time course, two excised-leaf studies using unlabeled HM and liquid chromatography–mass spectrometry analyses were performed. *Aegilops searsii* accumulated more HA than CS did, and each substitution line at 8, 12, and 24 h after treatment (HAT). Furthermore, only the wheat substitution line lacking chromosome 5A displayed greater abundance of HA relative to CS (2.4- to 3.8-fold, depending on the time point). In contrast, HA abundances in lines possessing chromosome 5A were not different than HA abundances in CS at all time points. When NT lines were compared with CS, the nullisomic 5D-tetrasomic 5A (N5D-T5A) line displayed similar HA abundance, whereas the nullisomic 5A-tetrasomic 5D (N5A-T5D) accumulated approximately 3-fold more HA at 12 and 24 HAT. These results biochemically support the hypothesis that genes encoding HA-detoxifying enzyme(s) are located on wheat chromosome 5A and corroborate findings from previous greenhouse phenotypic experiments. Future experimentation is needed to identify and characterize genes and enzymes on wheat chromosome 5A involved with HA detoxification, which may include cytochrome P450 monooxygenases, unknown oxidases, UDP-dependent glucosyltransferases, or, potentially, transcription factors that regulate expression of these genes associated with HA detoxification.

## Introduction

Halauxifen-methyl (HM) is categorized in the 6-aryl-picolinic acid subclass of synthetic auxin herbicides (Group 4) and was commercialized in 2015 (Epp et al. 2016; Schmitzer et al. 2015). Like other synthetic auxins, HM mimics indole-3-acetic acid, which regulates numerous aspects of plant growth and development (Demeulenaere and Beeckman 2014; McSteen 2010). Halauxifen-methyl provides selective postemergence control of dicot weeds in cereal crops (Dzikowski et al. 2016; Epp et al. 2016). While HM was initially developed as a tank-mix partner for postemergence weed control in cereal crops at relatively low application rates (5 to 7.5 g ha$^{-1}$), it can also be used as a burndown treatment before soybean [*Glycine max* (L.) Merr.] planting at even lower rates (1 to 2 g ha$^{-1}$) due to its short soil half-life (10 to 25 d) and minimal soil residual activity (Epp et al. 2016, 2018).

Allohexaploid bread wheat (*Triticum aestivum* L.) ($2n = 6x = 42$; AABBDD) is tolerant to HM via rapid detoxification of the biologically active form, halauxifen acid (HA) (Dzikowski et al. 2016) following phase I and II metabolic reactions. Phase I reactions typically involve oxidation, reduction, or hydrolysis of phytotoxic parent molecules; most reactions are catalyzed by cytochrome P450 enzymes (CYPs) or bioactivation of proherbicide esters by carboxylesterases (CXEs) (Gershater and Edwards 2007; Kreuz et al. 1996). Phase II reactions involve conjugation of phytotoxic parent molecules or phase I metabolites with endogenous compounds, such as sugars or reduced glutathione (Kreuz et al. 1996; Riechers et al. 2010). Following de-esterification of HM to HA, HA is *O*-demethylated and subsequently conjugated with glucose (Figure 1). Although HM metabolism in wheat has been characterized (Dzikowski et al. 2016), the genes encoding HA-detoxifying enzymes have not been identified. Identification of such genes would be valuable for plant transformation to endow HM tolerance in HM-sensitive plants, such as soybean (Zobiole and Kalsing 2017), cotton (*Gossypium hirsutum* L.), and other dicots. Additionally, these enzymes could potentially detoxify multiple herbicides,
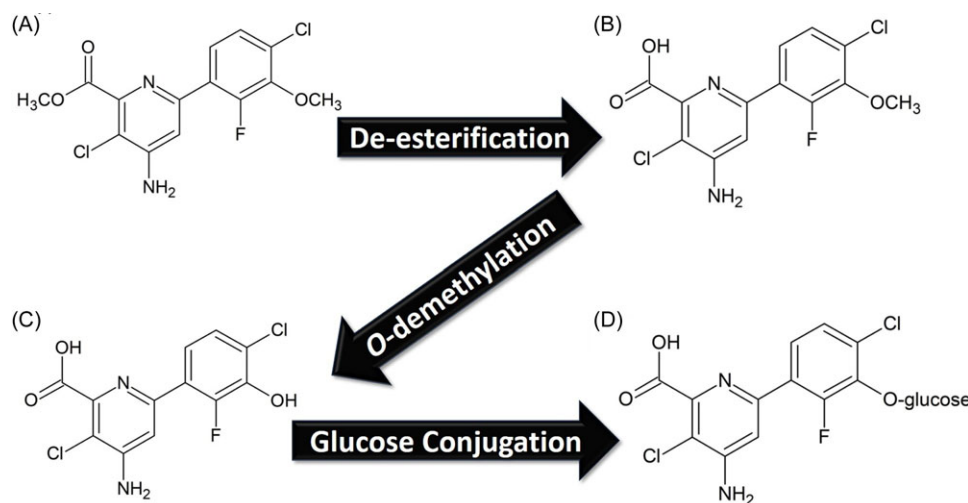
**Figure 1.** Structures of halauxifen-methyl (HM) and its metabolites in wheat: (A) HM; (B) halauxifen acid (HA); (C) *O*-demethylated metabolite of HA; and (D) glucose conjugate of HA.

making them valuable in breeding programs aimed at improving herbicide tolerance in dicot crops (Dimaano and Iwakami 2021; Gharabli et al. 2023).

Various genetic resources derived from the allohexaploid wheat cultivar 'Chinese Spring' (CS) are available for evaluating phenotypic responses via alteration of the base chromosome number or substituting chromosomes, including alien substitution and nullisomic-tetrasomic (NT) lines (Jiang et al. 1994; Law et al. 1987). Alien substitution lines have one pair of endogenous homoeologous chromosomes replaced with the homoeologous chromosomes from another species, denoted as the "alien" genome (Jiang et al. 1994). For NT lines, one pair of homoeologues are removed (nullisomic) and additional copies of another pair of homoeologues are added (tetrasomic) (Law et al. 1987; Sears 1954, 1966). These lines were utilized in previous HM phenotyping experiments with the goals of identifying lines with increased HM sensitivity and providing evidence concerning which chromosomes harbor genes necessary to confer HM tolerance in wheat (Obenland and Riechers 2020).

Increased sensitivity to HM was clearly evident in wheat lines that lack chromosome 5A, relative to CS (Obenland and Riechers 2020), but HM tolerance in wheat lines possessing 5A was similar to that of CS. In our prior research, we hypothesized that increased HM sensitivity in these wheat lines is due to reduced HA detoxification rates, which likely resulted from losing genes on chromosome 5A encoding HA-detoxifying enzymes (Obenland and Riechers 2020). To directly address this hypothesis, the objective of this study was to measure and compare HA levels in CS and wheat lines utilized in our previous research via a combination of excised-leaf assays and liquid chromatography–mass spectrometry (LC-MS) analysis.

## Materials and Methods

### Chemicals, Plant Materials, and Growth Conditions

Analytical-grade standards of HM and HA (95.9% and 99.5% pure, respectively) were provided by Corteva Agriscience (Indianapolis, IN, USA). All other analytical-grade reagents were purchased through Fisher Scientific (Thermo-Fisher, Hanover Park, IL, USA) or Sigma Chemical (Millipore Sigma, St Louis, MO, USA). Seeds for CS, alien substitution lines (5A, 5B, and 5D), and NT lines were

acquired from the Kansas State Wheat Genetics Resource Center; seed of Sears' goatgrass (*Aegilops searsii* M. Feldman & M. Kislev) (AS; PI 599163), a diploid wheat relative ($2n = 2x = 14$; S genome), was obtained from the National Small Grains Collection (Aberdeen, ID, USA) of the U.S. Department of Agriculture–Agricultural Research Service. To promote uniform germination, seeds were subjected to a cold treatment by placing them on water-soaked filter paper in Petri dishes stored at 5 C for 3 d. Seedlings were cultivated in a growth chamber (Conviron Gen1000, Controlled Environments, Winnipeg, Canada) until seedlings produced two to three leaves (Zadoks stage 12-13) under conditions of 28/22 C day/night and a 16/8-h photoperiod. The LED lights in the growth chamber provided 550 µmol m$^{-2}$ s$^{-1}$ photon flux at the plant canopy level.

### Excised-Leaf Assay, Tissue Harvest and Extraction, and LC-MS Analysis

The excised-leaf assay and metabolite extraction protocols utilized in our experiments are based on a protocol modified from previous studies (Concepcion et al. 2021; Lygin et al. 2018; Ma et al. 2015). For each experiment, the two oldest wheat leaves were cut at the collar, the cut surface of the leaf was washed with deionized water, transferred to 15-ml plastic tubes containing 400 µl of 0.1 M Tris-Cl (pH 6.0), and preincubated in the growth chamber for 1 h. After preincubation, leaves designated for HM treatment were transferred to tubes containing 400 µl of 300 µM HM (in 0.1 M Tris-Cl, pH 6.0) and untreated leaves were transferred to tubes containing only 400 µl of 0.1 M Tris-Cl (pH 6.0). Approximately 1.0 cm of tissue above the cut surface of the excised leaf was exposed to the uptake solution in these assays. At 2 h after treatment (HAT), leaves designated for the 2-HAT time point were rinsed with deionized water, and fresh weights were recorded (approx. 200 mg of fresh weight per sample). Samples designated for later time points (8, 12, and 24 HAT) were rinsed with deionized water and transferred to tubes containing 400 µl of quarter-strength Murashige and Skoog solution (MP Biomedicals, Solon, OH, USA), which provides mineral salts, vitamins, and organic compounds to support plant growth (Murashige and Skoog 1962). Following each harvest time point, leaves were frozen in liquid nitrogen, and samples were stored at −80 C until metabolite extraction. Based on preliminary experiments quantifying HM

remaining in the uptake solution at 2 HAT via high-performance liquid chromatography with photodiode array detection (HPLC-PDA) using methods (Supplementary Material 1) modified from a previous study (Concepcion et al. 2021), at least 19% of HM supplied was absorbed by excised wheat leaves (Supplementary Material 2). However, AS absorbed a greater amount of HM than CS, which may be related to anatomical differences between these species. Substitution line 5D and the nullisomic 5D-tetrasomic 5A (N5D-T5A) line also absorbed more HM than CS (Supplementary Material 2), which positively correlates with a relatively higher degree of HM tolerance (Obenland and Riechers 2020) and a putative faster rate of HM metabolism.

Frozen tissue was ground in liquid nitrogen using a mortar and pestle, and compounds were extracted in 1 ml of 90% (v/v) methanol. The supernatant was removed after centrifugation at $12,000 \times g$, and a second extraction was performed with the remaining plant material by adding 1 ml of 90% (v/v) methanol. After another centrifugation at $12,000 \times g$, the pellet was discarded, and the second supernatant was combined with the first supernatant, resulting in a final volume of 2 ml. All samples were spiked with 4-chloro-DL-PHE as an internal standard before extraction. Samples were dried and concentrated under nitrogen gas and reconstituted with 250 µl of water:acetonitrile (1:1, v/v) containing 0.1% formic acid. Quality-control (QC) samples were then prepared by combining aliquots of each sample for injection throughout each experimental run (Dunn et al. 2011). An HA standard was also prepared. All samples were stored at −80 C until further analysis.

Samples were submitted to the Roy J. Carver Metabolomics Facility, University of Illinois at Urbana-Champaign, for LC-MS analysis using previously described methods (Concepcion et al. 2021; Elolimy et al. 2019). Samples were analyzed with a Q-Exactive MS system (Thermo, Bremen, Germany), and separation was conducted with a Dionex Ultimate 3000 series HPLC equipped with a Phenomenex C18 column (4.6 by 100 mm, 2.6-µm particle size). Mobile phases consisted of A ($H_2O$ with 0.1% formic acid [v/v]) and B (acetonitrile with 0.1% formic acid [v/v]). The flow rate was 0.25 ml min$^{-1}$ with a linear gradient starting at 100% A for 3 min. The gradient then transitioned to 100% B (20 to 30 min) and returned to 100% A (31 to 36 min). Twenty microliters of each sample was injected, and the autosampler temperature was 15 C. Mass spectra were then acquired under both positive (sheath gas flow rate: 45; auxiliary gas flow rate: 11; sweep gas flow rate: 2; spray voltage: 3.5 kV; capillary temp: 250 C; auxiliary gas heater temp: 415 C) and negative electrospray ionization (sheath gas flow rate: 45; auxiliary gas flow rate: 11; sweep gas flow rate: 2; spray voltage: −2.5 kV; capillary temp: 250 C; auxiliary gas heater temp: 415 C). The full-scan mass-spectrum resolution was set to 70,000 with a scan range of $m/z$ 67 to 1,000, and the automatic gain control target was $1 \times 10^6$ with a maximum injection time of 200 ms. Chromatographic analysis was conducted in a randomized sequence, including QC samples injected initially to equilibrate the analytical platform and after every 10 test samples to evaluate the stability of the experimental procedure (Dunn et al. 2011; Godzien et al. 2015; Sangster et al. 2006; Wehrens et al. 2016). Raw data files obtained in full-MS mode (samples, procedural blank, and QC) and data obtained in full-MS followed by data-dependent MS2 were processed using MS-DIAL v. 4.9221218 following previously described parameters (Concepcion et al. 2021; Tsugawa et al. 2015). The peak area of each metabolite feature was normalized based on QC samples and peak area of the internal standard (Supplementary Material 2). Normalized peak areas for

HA were then exported into a .csv file for further statistical analysis.

### Experimental Setup and Statistical Analysis

The first experiment included CS, AS, and three alien substitution lines derived from CS wheat but with endogenous chromosomes 5A, 5B, or 5D replaced with the corresponding homoeologous chromosome (5S) from AS (Obenland and Riechers 2020). Based on the results of the first experiment, NT lines with different numbers of chromosomes 5A and 5D (i.e., 5A or 5D were either omitted [nullisomic] or doubled [tetrasomic]) were used for the second experiment, which included CS, nullisomic 5A-tetrasomic 5D (N5A-T5D), and N5D-T5A. Both experiments were designed to meet or exceed minimum requirements for replicating and reporting metabolite profiling results (Sumner et al. 2007). The first experiment was independently conducted twice using either three or four biological replicates per treatment per time point (seven total biological replicates). The second experiment was conducted once and utilized five biological replicates per treatment per time point. Chinese Spring served as a positive control in both experiments, as it is HM tolerant, while AS served as a negative control due to its sensitivity to HM (Obenland and Riechers 2020). Comparisons of HA normalized peak areas among populations and time points were performed with the LME4 package (Bates et al. 2015) in R (v. 4.2.0) using RStudio (v. 2023.03.0). Both experiments used a mixed-effects model in which population, time point, and their interactions were treated as fixed effects and replicates were random effects. Homogeneity of variance was confirmed with the Levene's test. Data were subjected to ANOVA, and treatment means were separated with Fisher's LSD ($\alpha = 0.05$).

## Results and Discussion

### LC-MS Analysis of HA Levels in CS, AS, Alien Substitution, and NT Lines

Peak abundances of HA in the first experiment with CS and AS exhibited anticipated results as positive and negative controls, respectively; the amounts of HA in CS remained relatively low throughout the time course, while HA peak abundances in AS increased during the time course and were greater than HA levels in CS and all substitution lines at 8, 12, and 24 HAT (Figure 2). At these same time points, HA levels in AS were 8.5-, 7.4-, and 5.6-fold higher, respectively, than HA levels in CS. Among substitution lines, only 5A accumulated HA relative to CS at 8, 12, and 24 HAT (Figure 2), with HA peak abundances 3.8-, 3.2- and 2.4-fold higher than HA levels in CS, respectively. In contrast, the level of HA in 5D was not different from HA levels in CS at any time point.

By comparison, HA levels in the 5B line (Figure 2) varied throughout the time course relative to CS, 5A, and 5D, which were more consistent between 8 and 24 HAT. The peak abundance of HA in 5B was not different from HA levels in CS or 5D at 8, 12, and 24 HAT, but HA abundance in 5B increased to levels also not different from HA levels in 5A at 12 and 24 HAT (Figure 2). This finding indicates the rate of HA metabolism in 5B at 12 and 24 HAT is slower than that in CS and 5D compared with its rate of metabolism at 8 HAT or, alternatively, that rates of HA formation from HM are higher in 5B at 12 and 24 HAT compared with 8 HAT. These metabolism results are in accord with previous phenotypic experiments in the greenhouse, where the 5B line displayed intermediate HM sensitivity relative to the highly sensitive 5A line and relatively tolerant 5D line (Obenland and
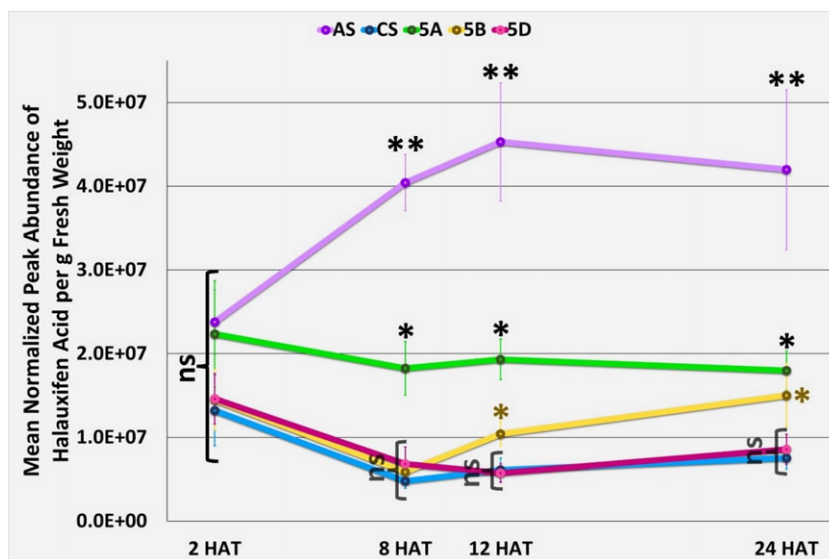
**Figure 2.** Mean normalized peak abundance of halauxifen acid (HA) in 'Chinese Spring' (CS) wheat, *Aegilops searsii* (AS), and wheat group 5 alien substitution lines 5A, 5B, and 5D. Means were determined from seven total biological replicates from two independent experiments at 2, 8, 12, and 24 h after treatment (HAT). Error bars represent the standard error of the mean. For each time point, means that are not significantly different are bracketed and marked "ns"; two asterisks (**) indicate a significant difference from all other means; a single black asterisk (*) indicates a significant difference from CS as well as means marked "ns"; and a single yellow asterisk (*) indicates means are not significantly different from CS, 5A, or 5D. Significant differences were determined using Fisher's LSD ($\alpha = 0.05$).

Riechers 2020). The variation in HA peak abundance in the 5B line during the time course may indicate competing CXE versus CYP enzyme activities (further described later), but additional research is needed to investigate this hypothesis. However, because HA peak abundances in lines 5A and 5D consistently differed at 8, 12, and 24 HAT, we focused on NT lines with varying numbers of 5A and 5D chromosomes (e.g., N5A-T5D and N5D-T5A) for subsequent LC-MS analysis.

In the second experiment, HA peak abundance in CS remained relatively low and did not significantly change throughout the time course (Figure 3), which was also noted in the previous experiment (Figure 2). Only line N5A-T5D displayed higher amounts of HA relative to CS at 12 and 24 HAT (approximately 3-fold; Figure 3). HA peak abundances in N5D-T5A did not differ from HA levels in CS throughout the time course (Figure 3).

These results indicate that species and lines lacking chromosome 5A (AS, N5A-T5D, and the 5A substitution line) have a relatively slow rate of HA metabolism. By contrast, lines possessing chromosome 5A (CS, N5D-T5A, and the 5B and 5D substitution lines) maintain HA metabolism rates similar to rates in CS. These findings support the hypothesis that genes encoding HA-detoxifying enzymes are located on wheat chromosome 5A, and as a result, lines lacking 5A consistently accumulate greater amounts of phytotoxic HA relative to lines possessing 5A through 24 HAT. Additionally, these results corroborate findings from previous greenhouse experiments in which 5A, N5A-T5D, and AS were relatively sensitive to HM, while CS, N5D-T5A, 5B, and 5D maintained tolerance to HM (Obenland and Riechers 2020).

As HM is absorbed by the cuticle and underlying leaf tissue, it is de-esterified to HA (Figure 1) at an unknown rate. HA is a phytotoxic, transient, phase I compound that is subsequently *O*-demethylated, then conjugated with glucose (Dzikowski et al. 2016; Figure 1). *O*-demethylation and glucose conjugation reactions are likely catalyzed by CYPs and UDP-dependent glucosyltransferases (UGTs), respectively, which commonly mediate synthetic auxin herbicide–detoxification reactions in

tolerant grasses (Frear 1995; Mithila et al. 2011; Sterling and Hall 1997; Zhang and Yang 2021). The presence of HA in all species and lines investigated (Figures 2 and 3) implies the activity of CXEs that convert HM to HA (Gershater and Edwards 2007). However, the activity of CXEs, CYPs, and UGTs and resulting metabolic flux could vary, which could shed more light on our current results. Given differential absorption of HM among some species and lines (Supplementary Material 2), future investigation of CXEs is warranted. For example, the abundance of HA in the 5B or 5D substitution lines during the time course (Figure 2) could be relatively low due to loss of an active CXE that converts HM to HA. Conducting a follow-up metabolism study and supplying HA instead of HM in our assay may help elucidate the possible role of differential CXE activity among wheat lines in future research.

Additional biokinetic analyses should also measure abundances of the *O*-demethylated metabolite and glucose conjugate of HA (Figure 1) to comprehensively understand altered HA detoxification rates or patterns in these substitution and NT lines. Such investigations would require analytical metabolite standards or radiolabeled HM, which were not available for the current study. Because these initial metabolites could be present but occur in low abundance—particularly the *O*-demethylated HA metabolite if it is rapidly turned over to phase II conjugates—a whole-plant assay may be more informative, especially if quantifying HM absorption, HA translocation, or measuring HA metabolites beyond 24 h is desired.

The discovery of HM sensitivity in AS was fortuitous for our prior research (Obenland and Riechers 2020). Detection of a relatively low HA metabolism rate (Figure 2) is notable because grasses are generally tolerant to synthetic auxins, with the exception of quinoline carboxylic acids (Grossmann 2010; Sterling and Hall 1997) and a different 6-aryl-picolinic acid herbicide, florpyrauxifen-benzyl (Epp et al. 2016; Lim et al. 2021; Miller et al. 2018; Takano et al. 2023). Interestingly, the wheat safener cloquintocet-mexyl (3.75 g ai ha$^{-1}$) reduced injury in AS even at an elevated rate of HM (60 g ae ha$^{-1}$ plus adjuvants; Obenland and Riechers 2020), which indicates enhancement of herbicide tolerance (presumably via
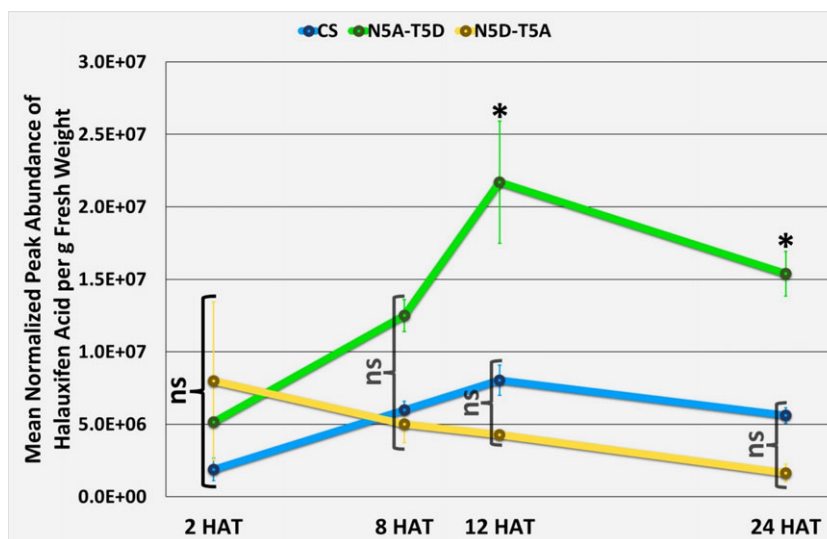
**Figure 3.** Mean normalized peak abundance of halauxifen acid (HA) in 'Chinese Spring' (CS) wheat and nullisomic-tetrasomic (NT) lines N5A-T5D and N5D-T5A. Means were determined from five biological replicates from one experiment at 2, 8, 12, and 24 h after treatment (HAT). Error bars represent the standard error of the mean. For each time point, means that are not significantly different are bracketed and marked "ns"; a single black asterisk (*) indicates a significant difference from CS and N5D-T5A. Significant differences were determined using Fisher's LSD ($\alpha = 0.05$).

induction of metabolic enzymes) by safeners is not limited to cultivated cereal crops (Riechers et al. 2010).

Our results inform future experiments, including RNA-seq or genome-wide association studies, aimed at identifying potential candidate genes on chromosome 5A. However, these experiments often yield numerous (>50) potential candidate genes (Baek et al. 2019). This is especially true for wheat, which has a relatively large (approximately 16 GB) allohexaploid genome (IWGSC 2018), meaning a significant gene might be identified along with its homoeologues. This concern is exacerbated since CYPs and UGTs are encoded by large multigene families per diploid genome (Casey and Dolan 2023; Gharabli et al. 2023). Previous studies utilizing various wheat species, alien substitution lines, or NT lines have identified differential homoeologous chromosome contributions to herbicide tolerance, metabolism, and gene expression patterns (Riechers et al. 1996, 1997; Xu et al. 2002; Yu et al. 2023).

Potential candidate genes encoding HA-detoxifying enzymes include CYPs and UGTs (Frear 1995; Mithila et al. 2011; Riechers et al. 2010; Zhang and Yang 2021). CYPs have been implicated in detoxification of numerous herbicides in the Poaceae, which has the highest number of herbicide-detoxifying plant CYPs (Brazier-Hicks et al. 2022; Casey and Dolan 2023; Dimaano and Iwakami 2021; Han et al. 2020; Pan et al. 2022; Yu et al. 2023; Zheng et al. 2022). Members of the plant CYP81A subfamily are the most common, but CYP72A and CYP71C members have also been identified (Supplementary Material 1). Compared with CYPs, genes encoding herbicide-detoxifying UGTs in plants are generally not as well characterized. UGT activities in wheat have been directly studied with natural product and xenobiotic substrates (Brazier et al. 2002), and the activities of herbicide-detoxifying UGTs have been inferred from metabolism studies in wheat in which glycosylated metabolites of isoproturon (Lu et al. 2015) and florasulam (DeBoer et al. 2006) were detected.

Regulatory elements and factors, such as promoters, untranslated regions (UTRs), and transcription factors (TFs), of candidate genes may also contribute to the prominent role of genes on wheat chromosome 5A in controlling HA detoxification compared with its homoeologous chromosomes 5B and 5D. The role of TFs in herbicide detoxification is often inferred, as RNA-seq has identified TFs regulated by herbicides and safeners (Baek et al. 2019; Brazier-Hicks et al. 2020; Chen et al. 2023; Duhoux et al. 2015; Gaines et al. 2014; Zhang et al. 2022). Homoeologue expression bias is commonly observed in allopolyploid plants (Grover et al. 2012), partly attributed to variations in *cis-* and *trans-* regulatory elements between homoeologues (He et al. 2022; Kremling et al. 2018). We therefore hypothesize potential candidate genes on chromosome 5A and their 5B and 5D homoeologues vary in promoter/UTR sequences and/or TF binding that regulates gene expression, resulting in relatively higher expression and activity of 5A homoeologues. However, gene copy number variation or differences in encoded protein sequences among homoeologous genes should not be precluded without further experimentation.

## References

Baek YS, Goodrich L V., Brown PJ, James BT, Moose SP, Lambert KN, Riechers DE (2019) Transcriptome profiling and genome-wide association studies reveal *GSTs* and other defense genes involved in multiple signaling pathways induced by herbicide safener in grain sorghum. Front Plant Sci 10:192

Bates D, Mächler M, Bolker BM, Walker SC (2015) Fitting linear mixed-effects models using lme4. J Stat Softw 67:1–48

Brazier M, Cole DJ, Edwards R (2002) *O*-glucosyltransferase activities toward phenolic natural products and xenobiotics in wheat and herbicide-resistant and herbicide-susceptible black-grass (*Alopecurus myosuroides*). Phytochemistry 59:149–156

Brazier-Hicks M, Franco-Ortega S, Watson P, Rougemont B, Cohn J, Dale R, Hawkes TR, Goldberg-Cavalleri A, Onkokesung N, Edwards R (2022) Characterization of cytochrome P450s with key roles in determining herbicide selectivity in maize. ACS Omega 7:17416–17431

Brazier-Hicks M, Howell A, Cohn J, Hawkes T, Hall G, McIndoe E, Edwards R (2020) Chemically induced herbicide tolerance in rice by the safener metcamifen is associated with a phased stress response. J Exp Bot 71:411–421

Casey A, Dolan L (2023) Genes encoding cytochrome P450 monooxygenases and glutathione *S*-transferases associated with herbicide resistance evolved before the origin of land plants. PLoS ONE 18:e0273594

Chen K, Su X, Yang H, Peng Y, Wu L, Zhao Z, Lin T, Bai L, Wang L (2023) Multi-omics analyses reveal the crosstalk between the circadian clock and the response to herbicide application in *Oryza sativa*. Front Plant Sci 14:1155258

Concepcion JCT, Kaundun SS, Morris JA, Hutchings SJ, Strom SA, Lygin AV, Riechers DE (2021) Resistance to a nonselective 4-hydroxyphenyl-pyruvate dioxygenase-inhibiting herbicide via novel reduction–dehy-dration–glutathione conjugation in *Amaranthus tuberculatus*. New Phytol 232:2089–2105

DeBoer GJ, Thornburgh S, Ehr RJ (2006) Uptake, translocation and metabolism of the herbicide florasulam in wheat and broadleaf weeds. Pest Manag Sci 62:316–324

Demeulenaere M, Beeckman T (2014) The interplay between auxin and the cell cycle during plant development. Pages 119–142 *in* Zažímalová E, Petrášek J, Benková E, eds. Auxin and Its Role in Plant Development. Vienna: Springer-Verlag

Dimaano N, Iwakami S (2021) Cytochrome P450-mediated herbicide metabolism in plants: current understanding and prospects. Pest Manag Sci 77:22–32

Duhoux A, Carrère S, Gouzy J, Bonin L, Délye C (2015) RNA-Seq analysis of rye-grass transcriptomic response to an herbicide inhibiting acetolactate-synthase identifies transcripts linked to non-target-site-based resistance. Plant Mol Biol 87:473–487

Dunn WB, Broadhurst D, Begley P, Zelena E, Francis-Mcintyre S, Anderson N, Brown M, Knowles JD, Halsall A, Haselden JN, Nicholls AW, Wilson ID, Kell DB, Goodacre R (2011) Procedures for large-scale metabolic profiling of serum and plasma using gas chromatography and liquid chromatography coupled to mass spectrometry. Nat Protoc 6:1060–1083

Dzikowski M, Becker J, Larelle D, Kamerichs B, Gast R (2016) Arylex™ active—new herbicide active and base for new cereals herbicides: Zypar™ and Pixxaro™ EC to control wide range of broadleaf weeds in cereals in Europe. Julius-Kühn-Archiv 452:297–304

Elolimy A, Alharthi A, Zeineldin M, Parys C, Helmbrecht A, Loor JJ (2019) Supply of methionine during late-pregnancy alters fecal microbiota and metabolome in neonatal dairy calves without changes in daily feed intake. Front Microbiol 10:2159

Epp JB, Alexander AL, Balko TW, Buysse AM, Brewster WK, Bryan K, Daeuble JF, Fields SC, Gast RE, Green RA, Irvine NM, Lo WC, Lowe CT, Renga JM, Richburg JS, *et al.* (2016) The discovery of Arylex™ active and Rinskor™ active: two novel auxin herbicides. Bioorg Med Chem 24:362–371

Epp JB, Schmitzer PR, Crouse GD (2018) Fifty years of herbicide research: comparing the discovery of trifluralin and halauxifen-methyl. Pest Manag Sci 74:9–16

Frear DS (1995) Wheat microsomal cytochrome P450 monooxygenases: characterization and importance in the metabolic detoxification and selectivity of wheat herbicides. Drug Metabol Drug Interact 12:329–358

Gaines TA, Lorentz L, Figge A, Herrmann J, Maiwald F, Ott MC, Han H, Busi R, Yu Q, Powles SB, Beffa R (2014) RNA-Seq transcriptome analysis to identify genes involved in metabolism-based diclofop resistance in *Lolium rigidum*. Plant J 78:865–876

Gershater MC, Edwards R (2007) Regulating biological activity in plants with carboxylesterases. Plant Sci 173:579–588

Gharabli H, Della Gala V, Welner DH (2023) The function of UDP-glycosyltransferases in plants and their possible use in crop protection. Biotechnol Adv 67:108182

Godzien J, Alonso-Herranz V, Barbas C, Armitage EG (2015) Controlling the quality of metabolomics data: new strategies to get the best out of the QC sample. Metabolomics 11:518–528

Grossmann K (2010) Auxin herbicides: current status of mechanism and mode of action. Pest Manag Sci 66:113–120

Grover CE, Gallagher JP, Szadkowski EP, Yoo MJ, Flagel LE, Wendel JF (2012) Homoeolog expression bias and expression level dominance in allopoly-ploids. New Phytol 196:966–971

Han H, Yu Q, Beffa R, González S, Maiwald F, Wang J, Powles SB (2020) Cytochrome P450 CYP81A10v7 in *Lolium rigidum* confers metabolic resistance to herbicides across at least five modes of action. Plant J 178:1081–1095

He F, Wang W, Rutter WB, Jordan KW, Ren J, Taagen E, DeWitt N, Sehgal D, Sukumaran S, Dreisigacker S, Reynolds M, Halder J, Sehgal SK, Liu S, Chen J, *et al.* (2022) Genomic variants affecting homoeologous gene expression dosage contribute to agronomic trait variation in allopolyploid wheat. Nat Commun 13:826

[IWGSC] International Wheat Genome Sequencing Consortium (2018) Shifting the limits in wheat research and breeding using a fully annotated reference genome. Science 361:eaar7191

Jiang JM, Friebe B, Gill BS (1994) Recent advances in alien gene-transfer in wheat. Euphytica 73:199–212

Kremling KAG, Chen SY, Su MH, Lepak NK, Romay MC, Swarts KL, Lu F, Lorant A, Bradbury PJ, Buckler ES (2018) Dysregulation of expression correlates with rare-allele burden and fitness loss in maize. Nature 555:520–523

Kreuz K, Tommasini R, Martinoia E (1996) Old enzymes for a new job: herbicide detoxification in plants. Plant Physiol 111:349–353

Law CN, Snape JW, Worland AJ (1987) Aneuploidy in wheat and its uses in genetic analysis. Pages 71–108 *in* Lupton FGH, ed. Wheat Breeding. Dordrecht, Netherlands: Springer

Lim SH, Kim H, Noh TK, Lim JS, Yook MJ, Kim JW, Yi JH, Kim DS (2021) Baseline sensitivity of *Echinochloa crus-gall* and *E. oryzicola* to florpyraux-ifen-benzyl, a new synthetic auxin herbicide, in Korea. Front Plant Sci 12:656642

Lu YC, Zhang S, Yang H (2015) Acceleration of the herbicide isoproturon degradation in wheat by glycosyltransferases and salicylic acid. J Hazard Mater 283:806–814

Lygin A V., Kaundun SS, Morris JA, Mcindoe E, Hamilton AR, Riechers DE (2018) Metabolic pathway of topramezone in multiple-resistant waterhemp (*Amaranthus tuberculatus*) differs from naturally tolerant maize. Front Plant Sci 9:1644

Ma R, Skelton JJ, Riechers DE (2015) Measuring rates of herbicide metabolism in dicot weeds with an excised leaf assay. J Vis Exp 103:e53236

McSteen P (2010) Auxin and monocot development. Cold Spring Harb Perspect Biol 2:a001479

Miller MR, Norsworthy JK, Scott RC (2018) Evaluation of florpyrauxifen-benzyl on herbicide-resistant and herbicide-susceptible barnyardgrass accessions. Weed Technol 32:126–134

Mithila J, Hall JC, Johnson WG, Kelley KB, Riechers DE (2011) Evolution of resistance to auxinic herbicides: historical perspectives, mechanisms of resistance, and implications for broadleaf weed management in agronomic crops. Weed Sci 59:445–457

Murashige T, Skoog F (1962) A revised medium for rapid growth and bio assays with tobacco tissue cultures. Physiol Plant 15:473–497

Obenland OA, Riechers DE (2020) Identification of chromosomes in *Triticum aestivum* possessing genes that confer tolerance to the synthetic auxin herbicide halauxifen-methyl. Sci Rep 10:8713

Pan L, Guo Q, Wang J, Shi L, Yang X, Zhou Y, Yu Q, Bai L (2022) CYP81A68 confers metabolic resistance to ALS and ACCase-inhibiting herbicides and its epigenetic regulation in *Echinochloa crus-galli*. J Hazard Mater 428:128225

Riechers DE, Irzyk GP, Jones SS, Fuerst EP (1997) Partial characterization of glutathione *S*-transferases from wheat (*Triticum* spp.) and purification of a safener-induced glutathione *S*-transferase from *Triticum tauschii*. Plant Physiol 114:1461–1470

Riechers DE, Kreuz K, Zhang Q (2010) Detoxification without intoxication: herbicide safeners activate plant defense gene expression. Plant Physiol 153:3–13

Riechers DE, Yang K, Irzyk GP, Jones SS, Fuerst EP (1996) Variability of glutathione *S*-transferase levels and dimethenamid tolerance in safener-treated wheat and wheat relatives. Pestic Biochem Physiol 56:88–101

Sangster T, Major H, Plumb R, Wilson AJ, Wilson ID (2006) A pragmatic and readily implemented quality control strategy for HPLC-MS and GC-MS-based metabonomic analysis. Analyst 131:1075–1078

Schmitzer PR, Balko TW, Daeuble JF, Epp JB, Satchivi NM, Siddall TL, Weimer MR, Yerkes CN (2015) Discovery and SAR of halauxifen methyl: a novel auxin herbicide. Pages 247–260 *in* Maienfisch P, Stevenson T, eds. Discovery and Synthesis of Crop Protection Products. Washington, DC: ACS Books

Sears ER (1954) The aneuploids of common wheat. Mo Agric Exp Stn Res Bull 572:1–58

Sears ER (1966) Nullisomic-tetrasomic combinations in hexaploid wheat. Pages 29–45 *in* Riley R, Lewis KR, eds. Chromosome Manipulations and Plant Genetics. Boston: Springer

Sterling TM, Hall JC (1997) Mechanism of action of natural auxins and the auxinic herbicides. Pages 111–141 *in* Roe R, Burton J, Kuhr R, eds. Herbicide Activity: Toxicology, Biochemistry and Molecular Biology. Amsterdam: IOS Press

Sumner LW, Amberg A, Barrett D, Beale MH, Beger R, Daykin CA, Fan TW-M, Fiehn O, Goodacre R, Griffin JL, Hankemeier T, Hardy N, Harnly J, Higashi R, Kopka J, *et al.* (2007) Proposed minimum reporting standards for chemical analysis. Metabolomics 3:211–221

Takano HK, Greenwalt S, Ouse D, Zielinski M, Schmitzer P (2023) Metabolic cross-resistance to florpyrauxifen-benzyl in barnyardgrass (*Echinochloa crus-galli*) evolved before the commercialization of Rinskor™. Weed Sci 71:77–83

Tsugawa H, Cajka T, Kind T, Ma Y, Higgins B, Ikeda K, Kanazawa M, Vandergheynst J, Fiehn O, Arita M (2015) MS-DIAL: data-independent MS/MS deconvolution for comprehensive metabolome analysis. Nat Methods 12:523–526

Wehrens R, Hageman JA, van Eeuwijk F, Kooke R, Flood PJ, Wijnker E, Keurentjes JJB, Lommen A, van Eekelen HDLM, Hall RD, Mumm R, de Vos RCH (2016) Improved batch correction in untargeted MS-based metabolomics. Metabolomics 12:88

Xu F-X, Lagudah ES, Moose SP, Riechers DE (2002) Tandemly duplicated safener-induced glutathione *S*-transferase genes from *Triticum tauschii* contribute to genome- and organ-specific expression in hexaploid wheat. Plant Physiol 130:362–373

Yu H, Guo X, Cui H, Chen J, Li X (2023) Metabolism difference is involved in mesosulfuron-methyl selectivity between *Aegilops tauschii* and *Triticum aestivum*. J Agric Food Chem 71:186–196

Zhang JJ, Yang H (2021) Metabolism and detoxification of pesticides in plants. Sci Total Environ 790:148034

Zhang Y, Gao H, Fang J, Wang H, Chen J, Li J, Dong L (2022) Up-regulation of *bZIP88* transcription factor is involved in resistance to three different herbicides in both *Echinochloa crus-galli* and *E. glabrescens*. J Exp Bot 73:6916–6930

Zheng T, Yu X, Sun Y, Zhang Q, Zhang X, Tang M, Lin C, Shen Z (2022) Expression of a cytochrome P450 gene from bermuda grass *Cynodon dactylon* in soybean confers tolerance to multiple herbicides. Plants 11:949

Zobiole LHS, Kalsing A (2017) Efficacy of halauxifen-methyl formulations to control volunteer soybean DAS-444Ø6-6 (Enlist E3™). Rev Bras Herb 16:192–197